JOURNAL OF VIROLOGY, Jan. 1979, p. 220-231
0022-538X/79/01-0220/12$02.00/0

Vol. 29, No. 1

Terminally Redundant Deletion Mutants of Bacteriophage BF23

A. R. SHAW,[1] D. LANG,[2] AND D. J. McCORQUODALE[1]*

Department of Biochemistry, Medical College of Ohio, Toledo, Ohio 43699,[1] and Biology Programs, The University of Texas at Dallas, Richardson, Texas 75080[2]

Received for publication 14 August 1978

Deletion mutants of bacteriophage BF23 were isolated and the positions of the deletions were determined. Two different deletable regions were detected: one in the same region as previously reported for bacteriophage T5, which is closely related to BF23; and the other within both terminal repetitions. The former deletable region lay between positions 0.31 and 0.36, which represented the fractional lengths of the BF23(+) DNA as measured from its left end. The latter deletion was evenly divided between the two terminal repetitions. The deletion in the left terminal repetition lay between positions 0.044 and 0.078 and was repeated in the corresponding region of the right terminal repetition between positions 0.966 and 1.0. The size of the DNA transferred to host cells during the first step of DNA transfer by BF23 carrying deletions in the terminal repetitions of its DNA was less than the size of DNA transferred during the first step by wild-type BF23 by an amount equal to the size of the deletion in each terminal repetition. This finding suggests the existence of a specific mechanism for delineating the position at which the first step of DNA transfer is stopped.

Bacteriophages BF23 and T5 are closely related and therefore have many structural and physiological properties in common (14). The DNA in mature particles of both phages has a molecular weight close to 77×10^6 and is a linear duplex molecule with a large terminal redundancy of about 6.5 megadaltons (Mdal) and with single-stranded nicks that are non-randomly distributed and repairable with ligase (4, 11). The DNA of both phages is transferred to host cells in a two-step process. A terminally redundant end is transferred first (the first-step-transfer DNA or FST DNA), and only after certain genes in the FST DNA are expressed is the remainder of the phage DNA transferred. Up to 10% of the DNA of T5(+) can be deleted from a region of the DNA between 0.216 and 0.324 of the fractional length of the molecule measured from the left end (see Fig. 4) without affecting its viability in common laboratory hosts (25). Such deletion mutants are termed *st* mutants because they are more *s*table at elevated *t*emperatures in saline-citrate buffer than is T5(+) (1, 3, 10).

We demonstrate in this paper that the DNA of BF23 not only can be deleted in the same region as reported for the DNA of T5, but also can be deleted in an entirely different region, namely within the terminally redundant ends, without affecting viability in common laboratory hosts. Based upon electrophoretic patterns of single-stranded DNA fragments from BF23(+) and its deletion mutants, and upon heteroduplex mapping of DNA from deletion mutants, a model for the distribution of single-strand nicks in BF23 DNA is presented. Furthermore, a BF23 mutant with a deletion within its terminally redundant ends is shown to transfer significantly less DNA to host cells during the first step of DNA transfer than does BF23(+).

(The results in this paper were reported at the Cold Spring Harbor meeting on bacteriophages, Cold Spring Harbor, New York, August 1977.)

MATERIALS AND METHODS

Source of bacteria and bacteriophages. Bacteriophage BF23(+) and its host, *Escherichia coli* W3110, have been described previously (16), as has T5(+) (13).

Growth of bacteria and bacteriophages. *E. coli* W3110 used for seeding plates was grown at 37°C in nutrient broth (2). Stocks of BF23 were prepared from plates containing nutrient agar plus 1 mM $CaCl_2$ that had been seeded with sufficient BF23 and *E. coli* 3110 to yield almost confluent lysis of the bacterial lawn (2). ^{32}P-labeled BF23 was prepared as follows. *E. coli* W3110 was grown in morpholinopropane sulfonate (MOPS) medium at pH 7.4 (17) at 37°C with one-third the standard phosphate concentration. When the culture reached a concentration of 2.4×10^7 cells per ml, 5 BF23 phage particles were added per 100 bacterial cells, and [^{32}P]orthophosphate (Schwarz/Mann no. 0063-22) was added to give a final concentration of 10 μCi/ml. The infected culture was incubated at 37°C

for 3 h, and the ^{32}P-labeled phage was isolated by differential ultracentrifugation.

Isolation of BF23 deletion mutants. Deletion mutants of BF23 were isolated by a modification of the procedure of Hertel et al. (10). A stock of BF23(+) was diluted to a concentration of 1×10^7 phage per ml in citrate buffer (0.01 M sodium citrate, 0.4 M NaCl, and 0.01% gelatin, pH 6.8) and heated at 64°C for 15 min. A stock was prepared from the surviving phage and was diluted in citrate buffer in preparation for another heat treatment. This cycle was repeated two more times. The stock prepared from phage that survived the third heat treatment was banded in a CsCl gradient to equilibrium. Fractions collected from the gradient were titered, and single plaques were picked from fractions in the peak of lowest buoyant density. Stocks grown from these single plaques were banded isopycnically in CsCl gradients with wild-type BF23 to test for differences in buoyant density. Stocks displaying buoyant densities less than that of wild-type BF23 were studied further.

Isolation of DNA. DNA was prepared by the phenol-sodium dodecyl sulfate (SDS) extraction method of Chen (6). Phage stocks were diluted 1:2 in buffer containing 0.05 M Tris (pH 7.5) and 0.2% SDS. An equal volume of distilled phenol saturated with 0.1 M Tris at pH 7.5 was added. This mixture was agitated gently on a clinical rotor at room temperature for 15 min and then centrifuged at room temperature for 10 min at $2,000 \times g$. The phenol layer was removed, an equal volume of fresh phenol was added, and the mixture was agitated for another 15 min. After centrifugation, a third phenol-SDS extraction was performed. The final aqueous layer containing the DNA was removed with a large-bore Pasteur pipette and dialyzed against four changes of 100 volumes of 0.01 M Tris (pH 7.5) containing 0.1 M KCl and 0.005 M EDTA.

Electrophoresis of single-stranded DNA in agarose gels. Isolated DNA was denatured before electrophoresis in 0.1 M NaOH containing 10% sucrose. Electrophoresis was carried out in 0.6 or 1.0% agarose gels. Electrode buffer consisted of 0.04 M Tris containing 0.005 M sodium acetate and 0.001 M EDTA at pH 7.8. Gels were run at 4°C for 20 h at 3 mA per tube or 17 mA per slab. Tube gels were 0.5 inch (ca. 1.2 cm) in diameter and 20 cm long. Slab gels were 1 cm thick, 12 cm long, and 18 cm wide with a 1-cm 15% polyacrylamide plug across the bottom. Gels were stained with ethidium bromide (5 μg/ml) for 2 h and destained in water for 2 h. Bands were visualized under UV light from a UVS-54 Mineralight.

Length determination of FST DNA fragments. *E. coli* W3110 was grown in nutrient broth plus 1 mM $CaCl_2$ at 37°C to 3.5×10^8 cells per ml, sedimented at 4°C for 10 min at $12,000 \times g$ (8,500 rpm in a Sorvall GSA rotor), washed in MOPS buffer (MOPS medium without glucose), and suspended in MOPS buffer at a concentration of 5×10^{10} cells per ml. After starvation of the cells for 30 min at 37°C without aeration, ^{32}P-labeled phage was added at an input ratio of 10 phages per cell and allowed to adsorb for 15 min. The infected cells were diluted 1:1 in cold MOPS buffer and blended in a Sorvall Omnimixer at maximum speed for 12 min at 0°C. The bacteria-FST complexes were centrifuged at $12,000 \times g$ for 10 min, and the resulting pellet was washed twice in MOPS buffer by resuspension and sedimentation. DNA was extracted by the phenol-SDS method, dialyzed against 4 changes of 100 volumes of 0.05 M sodium phosphate at pH 6.7 containing 0.1 M NaCl, and layered atop a 10 to 30% sucrose gradient containing 0.05 M sodium phosphate at pH 6.7 and 0.1 M NaCl. The samples were centrifuged at 14°C in an SW 25.1 rotor for 25 h at 22,000 rpm. Fractions containing the most FST DNA were pooled and prepared for electron microscopy.

Contour length measurements by electron microscopy. FST-DNA was prepared for electron microscopy by spontaneous adsorption from 0.2 M ammonium acetate according to Lang and Mitani (12). Electron micrographs were projected at a magnification of 23.7, and the contour length of the DNA molecules was measured with a linear integrator (Numonics Corp.).

Heteroduplex mapping. Single-strand interruptions in the DNA of BF23(+), BF23*st*(4), and BF23*st*(9) were sealed with T4 ligase (Miles 39-625) by the method of Rhoades and Rhoades (21). Heteroduplexes of DNA from BF23*st*(4) and BF23*st*(9) were produced by the formamide technique of Davis et al. (7), and prepared for electron microscopy as follows. A 0.05-ml portion of a solution of heteroduplex DNA in 0.01 M phosphate buffer and 0.001 M EDTA at pH 7.8 plus 0.025 ml of 37% formaldehyde were heated in a test tube for 5 min at 35°C. This treatment expands single-stranded DNA without denaturing double-helical regions. At the end of the heating period, the following components were added to the heteroduplex DNA solution in this sequence: 2.66 ml of ice-cold water, 2.20 ml of 2 M NH_4Cl containing 0.01 M EDTA, and 0.07 ml of 0.01% cytochrome *c*. From this solution, droplets of about 0.04 ml were put on Teflon and sampled for electron microscopy according to the spontaneous adsorption method of Lang and Mitani (12), and then rotary shadowed with platinum. Micrographs were taken at 80 kV with a Siemens Elmiskop IA at a magnification of 5×10^3, calibrated with carbon replicas of a cross-lined optical grating (2,160 lines/mm; E. F. Fullam, Inc.). Contour lengths of DNA molecules were measured as described above. Lengths of single-stranded DNA regions were multiplied by 1.26 to correct for longitudinal contraction.

RESULTS

We isolated 10 mutants of BF23 that are more resistant to inactivation by heating under the conditions described above than is wild-type BF23. These mutants have buoyant densities in CsCl less than that of BF23(+), and we have designated them *st*(1), *st*(2), *st*(3), *st*(4), *st*(5), *st*(6), *st*(7), *st*(8), *st*(9), and *st*(10). The contour length of the DNA from both BF23*st*(4) and BF23*st*(9) is less than that from BF23(+) (Table 1 [13]). Hence, BF23*st*(4) and BF23*st*(9) are deletion mutants, and on the basis of the lower buoyant densities and the electrophoretic patterns of denatured DNA from the other mutants,

TABLE 1. *Contour lengths of DNA from BF23(+), BF23st(4), BF23st(9), and of regions of heteroduplex DNA (H-DNA) formed from BF23st(4) and BF23st(9)*

Source of DNA	Length			Fraction of BF23(+) DNA			Mol wt[c] (millions)	No. of base pairs[d] (Kbp)
	(μm)	± SSD[a]	± SDM[b]	%	± SSD	± SDM		
BF23(+)	37.03	0.83	0.13	100	2.2	0.4	76.7	116
BF23*st*(4)	34.51	0.69	0.12	93.2	2.5	1.0	71.5	108
BF23*st*(9)	35.12	0.71	0.13	94.8	2.3	0.9	72.7	110
H-DNA region 1[e]	1.64	0.14	0.06	4.43	0.38	0.16	3.39	5.13
H-DNA region 2	1.26	0.15	0.05	3.40	0.40	0.13	2.61	3.94[f]
H-DNA region 3	8.51	0.35	0.13	22.98	0.95	0.35	17.62	26.62
H-DNA region 4	1.91	0.18	0.06	5.16	0.49	0.16	3.95	5.97[f]
H-DNA region 5	22.45	0.22	0.11	60.63	0.59	0.30	46.47	70.22
H-DNA region 6	1.26	0.34	0.18	3.40	0.92	0.50	2.61	3.94[f]

[a] SSD, Sample standard deviation ($\sqrt{\Sigma(\bar{x} - x)^2}/\sqrt{N-1}$).
[b] SDM, Standard deviation of the mean (SSD/$\sqrt{N}$).
[c] Molecular weight = 2.07 ($\times 10^6$/μm) × length (μm) (13).
[d] Number of 1,000 base pairs = 3.128 (Kbp/μm) × length (μm).
[e] Regions of the heteroduplex DNA are defined in the legend to Fig. 7.
[f] If double stranded.

we conclude that these other mutants also have deletions in their DNA.

The electrophoretic pattern of single-stranded DNA fragments from BF23(+) is remarkably similar to that from T5(+) (Fig. 1). However, two obvious differences can be seen between the two patterns. First, the 8.1-Mdal fragment of T5(+) is considered a minor fragment (9) and has a different molecular weight than the analogous 7.9-Mdal fragment of BF23(+), which we consider to be a major fragment. Furthermore, if the molecular weight of the 7.9×10^6 fragment is added to the molecular weights of the other major fragments that have molecular weights from 3.07×10^6 to 13.3×10^6, the sum is greater than the expected 38.15×10^6, which is considered to be the molecular weight of the uninterrupted strand of the duplex DNA molecule, by exactly 7.9×10^6. We conclude therefore that the 7.9-Mdal fragment arises from the 13.3-Mdal fragment by a nick that divides the 13.3×10^6 fragment into a 7.9-Mdal fragment and a 5.4-Mdal fragment. The 5.4-Mdal fragment in the agarose gel therefore consists of two species of molecules that arise from different locations in the duplex DNA molecule. The nick in the 13.3-Mdal fragment, however, does not occur in all DNA molecules, and therefore the DNA in a population of BF23(+) particles consist of two major types, one with and one without a nick in the 13.3-Mdal fragment.

The second obvious difference between the electrophoretic patterns of single-stranded DNA fragments from BF23(+) and T5(+) is the size and relative frequency of those single-stranded DNA fragments with molecular weights of 3.07×10^6 and less. In the T5(+) pattern, four minor bands with molecular weights of 3.0×10^6, 2.7×10^6, 2.2×10^6, and 1.8×10^6 and one major band with a molecular weight of 1.6×10^6 are found (9). In the BF23(+) pattern, fragments with molecular weights of 3.07×10^6, 2.67×10^6, 2.29×10^6, and 2.07×10^6 are found in approximately equal numbers.

The electrophoretic patterns of the denatured DNA from our deletion mutants are of three types (Fig. 2). One type is represented by BF23*st*(9) and includes BF23*st*(5). Another type is represented by BF23*st*(4) and includes BF23*st*(2), -*st*(3), -*st*(6), -*st*(7), -*st*(8), and -*st*(10). The third type is represented by BF23*st*(1). The BF23*st*(9) pattern is very similar to that of T5*st*(0), which has a deletion between 0.268 and 0.324 of the fractional length of wild-type T5 DNA as measured from its left end (see Fig. 4). The molecular weights of the single-stranded DNA fragments from BF23(+), BF23*st*(9), and BF23*st*(4) have been estimated from the known molecular weights of single-stranded fragments from T5 (Fig. 1 and 3; see also references 8 and 9). Based upon these molecular weights and upon analogy to the arrangement of DNA fragments in T5(+) and T5*st*(0), a model for the arrangement of single-stranded DNA fragments in BF23(+) and BF23*st*(9) is presented in Fig. 4.

The model for BF23*st*(9) agrees very well with the conclusion that the deletion in its DNA eliminates a portion from the 13.3-Mdal and the 5.4-Mdal fragments of BF23(+) DNA, thereby eliminating the nick between them. Such a deletion would produce two new fragments, one with a molecular weight greater than that of the 13.3×10^6 fragment and the other with a molecular weight greater than either of the 5.4×10^6 fragments. The difference between 18.7-Mdal (13.3 Mdal plus 5.4 Mdal) and the larger of the two

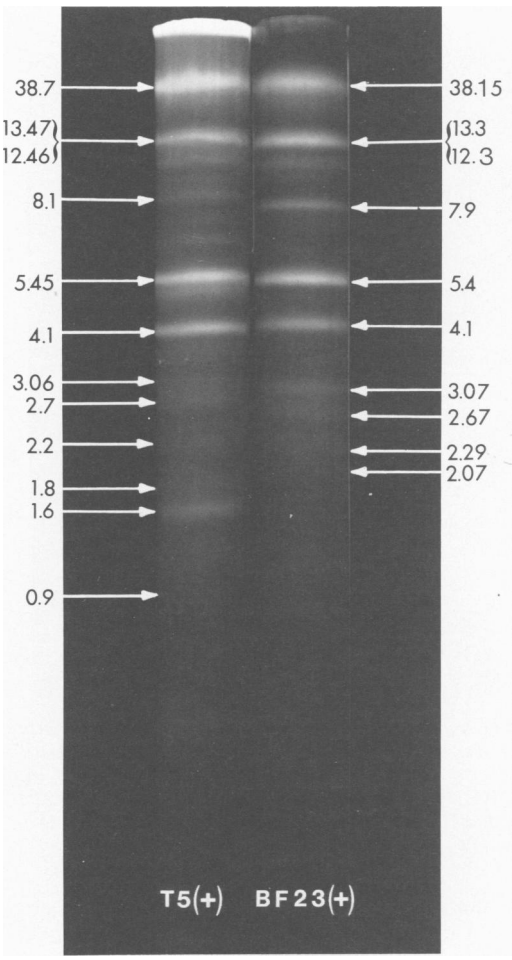

FIG. 1. *Electrophoretic separation of single-stranded DNA fragments from BF23(+) and from T5(+). DNAs extracted from BF23(+) and T5(+) were denatured with 0.1 M NaOH, and the resulting single-stranded fragments were separated by electrophoresis on 0.6% agarose tube gels as described in the text. Samples are T5(+) (left) and BF23(+) (right).*

new fragments (16.8 Mdal) is 1.9 Mdal. The difference between 10.8 Mdal (5.4 Mdal plus 5.4 Mdal) and the smaller of the two new fragments (8.9 Mdal) is also 1.9 Mdal. Two times 1.9 Mdal (i.e., 3.8 Mdal) is the total amount of double-stranded DNA deleted from each BF23*st*(9) particle (Fig. 4). In addition, as would be predicted, both 5.4-Mdal fragments disappeared from the DNA of BF23*st*(9) (Fig. 2).

The electrophoretic pattern of single-stranded DNA fragments from BF23*st*(4) is different from any previously observed pattern of DNA fragments from either BF23 (Fig. 5) or T5. First, the 12.3×10^6 fragment was shortened to 11.1×10^6, and no other major fragment with a molecular weight above 3.07×10^6 was affected except the 38.15×10^6 fragment, which represents the uninterrupted strand of the whole duplex DNA molecule from BF23(+). Second, the four fragments with molecular weights of 3.07×10^6, 2.67×10^6, 2.29×10^6, and 2.07×10^6 are not present in BF23*st*(4) DNA. In their place are fragments with molecular weights of 1.84×10^6, 1.44×10^6, 1.06×10^6, and 0.84×10^6. Clearly, the deletion in BF23*st*(4) has affected the molecular weights of these relatively small fragments. Since the analogous small fragments from T5 arise because of nicks in its terminally repetitious DNA, we surmise that the small fragments of BF23 DNA arise similarly. The difference in molecular weight between 3.07×10^6 and 1.84×10^6, between 2.67×10^6 and 1.44×10^6, between 2.29×10^6 and 1.06×10^6, and between 2.07×10^6 and 0.84×10^6 is, in each case, 1.23×10^6. If a deletion of 4.92 Mdal were divided equally between each terminal redundancy, we would expect one-half of 2.46 or 1.23 Mdal of DNA less in certain single-stranded DNA fragments from BF23*st*(4). Hence, the amount of DNA deleted from BF23(+) to yield BF23*st*(4) (4.92 Mdal) determined in this way is compatible with the amount deleted as measured by total contour lengths (5.2 ± 2.1 Mdal) (Table 1).

To confirm that the deletion in the DNA of BF23*st*(4) is equally divided between its two terminal redundancies, we prepared heteroduplexes between ligated DNA of BF23*st*(4) and that of BF23*st*(9). In such heteroduplexes, the left and right ends of the DNA molecules can be determined by noting the location of the loop of single-stranded DNA from BF23*st*(4) that has no complementary region in the DNA from BF23*st*(9). The deletion in the DNA from BF23*st*(9) is in the left half of the molecule in the region between 0.31 and 0.36 of the fractional length of DNA from BF23(+) as measured from the left end of the heteroduplexes (Fig. 6a). The region deleted in BF23*st*(9) overlaps the deletable region in T5(+) DNA, which is between 0.22 and 0.32 of the fractional length from its left end (25), and includes the nick at position 0.33 of BF23(+) DNA. These findings confirm our previous conclusion that the nick at position 0.33 is deleted in BF23*st*(9) DNA and support our model for BF23*st*(4) and BF23*st*(9) DNA presented in Fig. 4. The left end of a heteroduplex between BF23*st*(4) and BF23*st*(9) DNAs is shown in Fig. 6a and displays one single-strand loop of a length corresponding to positions 0.044 through 0.078, and another corresponding to positions 0.31 through 0.36 (Fig. 7; Table 1). The latter loop is due to the deletion in BF23*st*(9) and defines the left half of the molecule, whereas

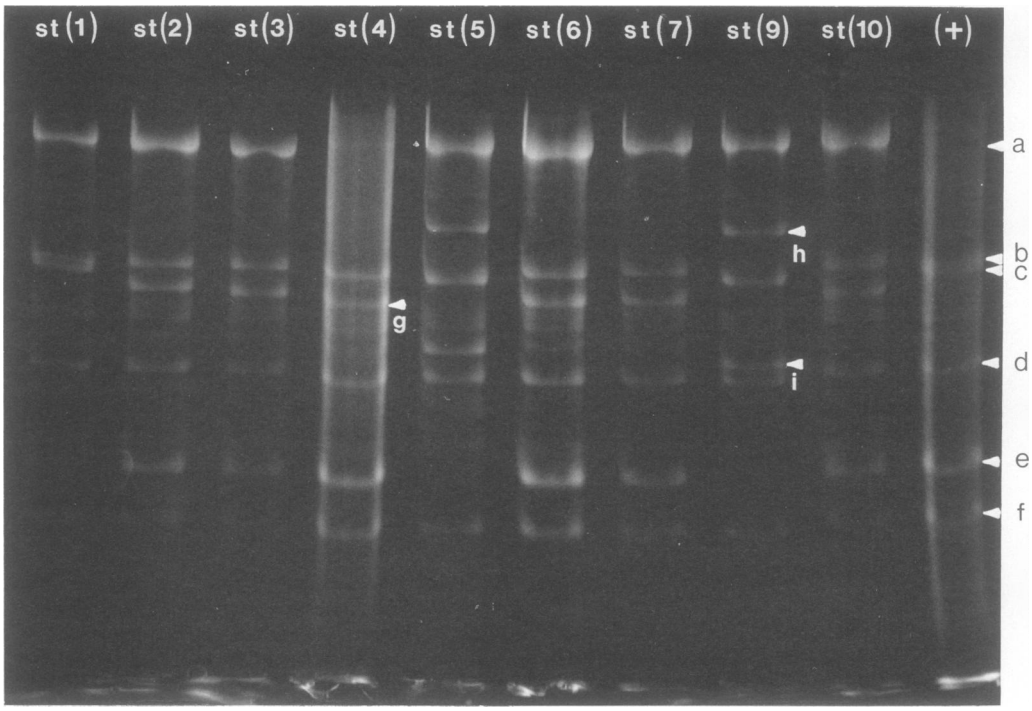

FIG. 2. *Electrophoretic separation of single-stranded DNA fragments from BF23 and its deletion mutants. DNAs extracted from BF23(+) and nine deletion mutants were denatured with 0.1 M NaOH, and the resulting single-stranded fragments were separated by electrophoresis on a 0.6% agarose slab gel as described in the text. Samples are, from left to right, BF23st(1), BF23st(2), BF23st(3), BF23st(4), BF23st(5), BF23st(6), BF23st(7), BF23st(9), BF23st(10), and BF23(+). The letters beside the arrowheads correspond to the following molecular weights in millions: a, 38.15; b, 13.3; c, 12.3; d, 7.9; e, 5.4; f, 4.1; g, 11.1; h, 16.8; and i, 8.9.*

the former loop is due to the deletion in BF23*st*(4) and shows that it is in the right half of the left terminal redundancy. The right end of the same heteroduplex shown in Fig. 6a is shown in Fig. 6b and displays not a loop but a terminal segment of single-stranded DNA that has a length equal to that of the loop at the far left end of the heteroduplex (Fig. 7; Table 1). These results clearly demonstrate that the deletion in BF23*st*(4) consists of two equal deletions of 2.46 Mdal from the same region of each terminal DNA redundancy, and that the rightward limit of the deletion in the terminal redundancy at the left end of the molecule is close to or at the internal limit of the left terminal redundancy itself. Consequently, the rightward limit of the deletion in the terminal redundancy at the right end of the molecule is close to or at the right terminus of the whole DNA molecule. The finding that the molecular weight of the 4.1×10^6 fragment, which is adjacent to the left terminal redundancy, is not affected by the deletion in BF23*st*(4) (Fig. 4) must mean that the deletion does not include the major nick at position 0.08. Since we find a single-stranded region rather than a loop or an uneven Y-structure at the right end of heteroduplexes between BF23*st*(4) and BF23*st*(9) DNAs, the length of which is exactly equal to the loop near the left end that is due to the deletion in the left terminal redundancy of BF23*st*(4) DNA, it appears that little if any of the left end of the 4.1-Mdal fragment contributes to the left terminal redundancy. The nick at position 0.08 must therefore be at or very close to the internal limit of the left terminal redundancy, and its corresponding position at the right end of the DNA must coincide with or be extremely close to the physical right end of the BF23 DNA.

The above findings support the models for the location of nicks in BF23(+), BF23*st*(9), and BF23*st*(4) that are proposed in Fig. 4. In the model of the DNA of BF23(+), a major nick at position 0.08 and three minor nicks at positions 0.01, 0.02, and 0.026 are placed in the terminal redundancy at the left end of the molecule. Nicks in analogous positions are also placed in the terminal redundancy at the right end of the molecule. The positions of these nicks are chosen to be similar but not identical to some found in

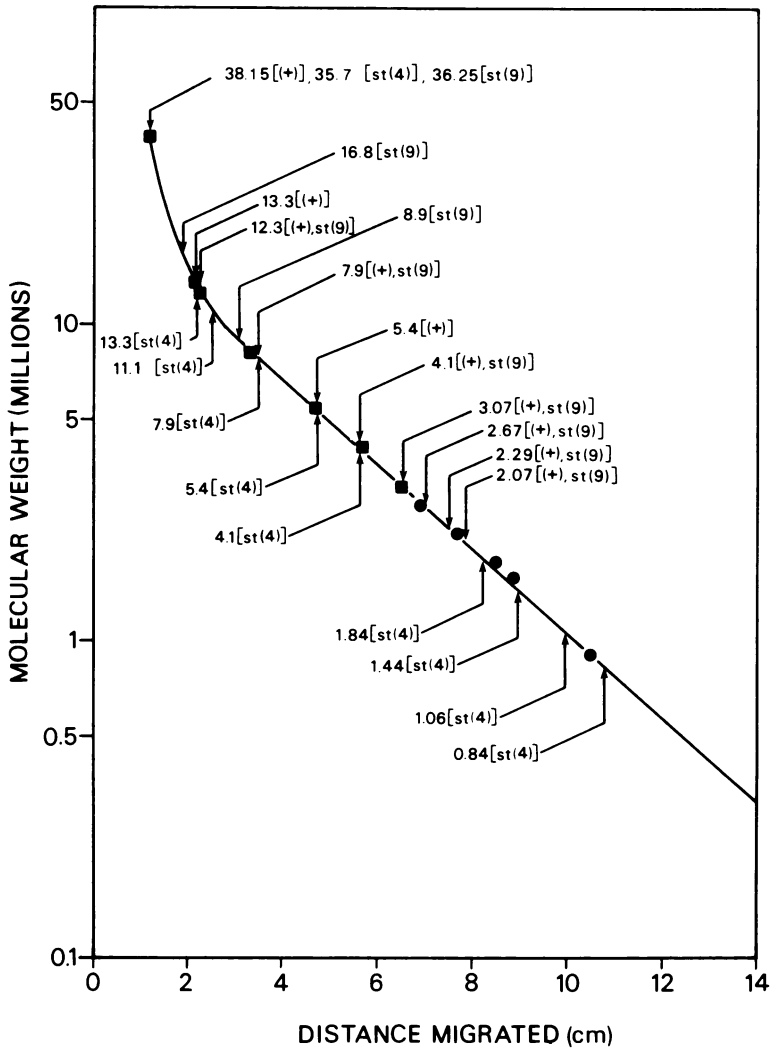

FIG. 3. *Relationship between molecular weight of single-stranded DNA fragments and electrophoretic mobility. The molecular weights of major single-stranded fragments from denatured T5(+) DNA were used as reference standards and were taken from Hayward and Smith (●) (9) or were calculated from Hamlett et al. (■) (8) by multiplying the fractional length of each major fragment by one-half of the molecular weight of double-stranded wild-type T5 DNA (77.4 × 10^6) as determined by Lang et al. (13). The arrows show the positions to which single-stranded DNA fragments from BF23(+), BF23st(4), and BF23st(9) migrated relative to the reference fragments. The values beside each arrow represent the interpolated molecular weights of DNA fragments from BF23 in millions.*

the left and right terminal redundancies of T5 DNA (20, 26) and to make them compatible with the molecular weights of the single-stranded DNA fragments that originate from the terminal redundancies in the DNA from both BF23(+) and BF23*st*(4).

With the establishment of a deletion in the redundant ends of BF23 DNA, a question arises as to the effect of this deletion on the first step of DNA transfer. Is the amount of DNA initially transferred to host cells by BF23*st*(4) the same or less than that transferred by BF23(+)? BF23(+) or BF23*st*(4) were adsorbed to host cells under conditions that permitted only the first step of DNA transfer to occur (see above), and the resulting complexes were mechanically sheared to yield host cells containing only the phage DNA that could be transferred in the absence of gene expression (the FST DNA). The FST DNAs from both BF23(+) and BF23*st*(4)

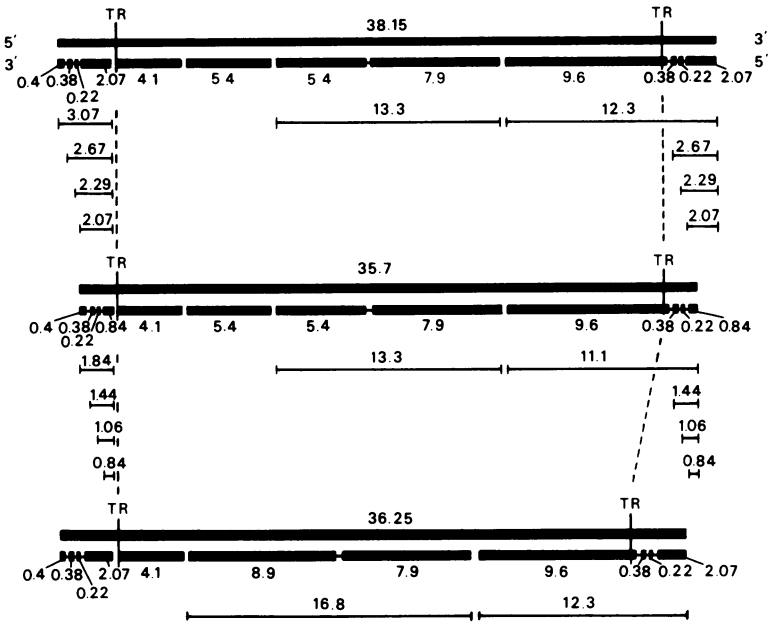

FIG. 4. *Arrangement of single-stranded DNA fragments in the chromosomes of BF23(+), BF23st(4), and BF23st(9). Duplex DNA molecules are represented by heavy double lines. Major nicks are shown as interruptions in one of the heavy lines. Minor nicks are shown as constrictions in one of the heavy lines. Locations of fragments resulting from the presence or absence of minor nicks are represented by lines below each duplex. TR defines the internal limits of terminal redundancies. Molecular weights of single-stranded fragments are in millions.*

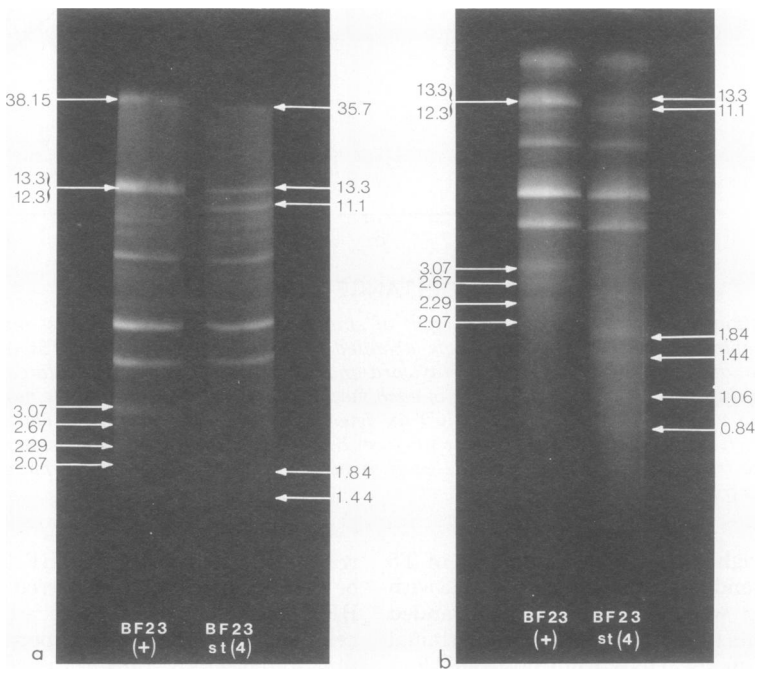

FIG. 5. *Electrophoretic separation of single-stranded DNA fragments from BF23st(4). DNAs extracted from BF23(+) and BF23st(4) were denatured with 0.1 M NaOH, and the resulting single-stranded DNA fragments were separated by electrophoresis on agarose tube gels as described in the text. (a) Single-stranded DNA from BF23(+) (left) and BF23st(4) (right) separated by electrophoresis on 0.6% agarose tube gels for analysis of single-stranded fragments larger than 4 Mdal. (b) Single-stranded DNA from BF23(+) (left) and BF23st(4) (right) separated by electrophoresis on 1.0% agarose tube gels for analysis of single-stranded fragments smaller than 4 Mdal.*

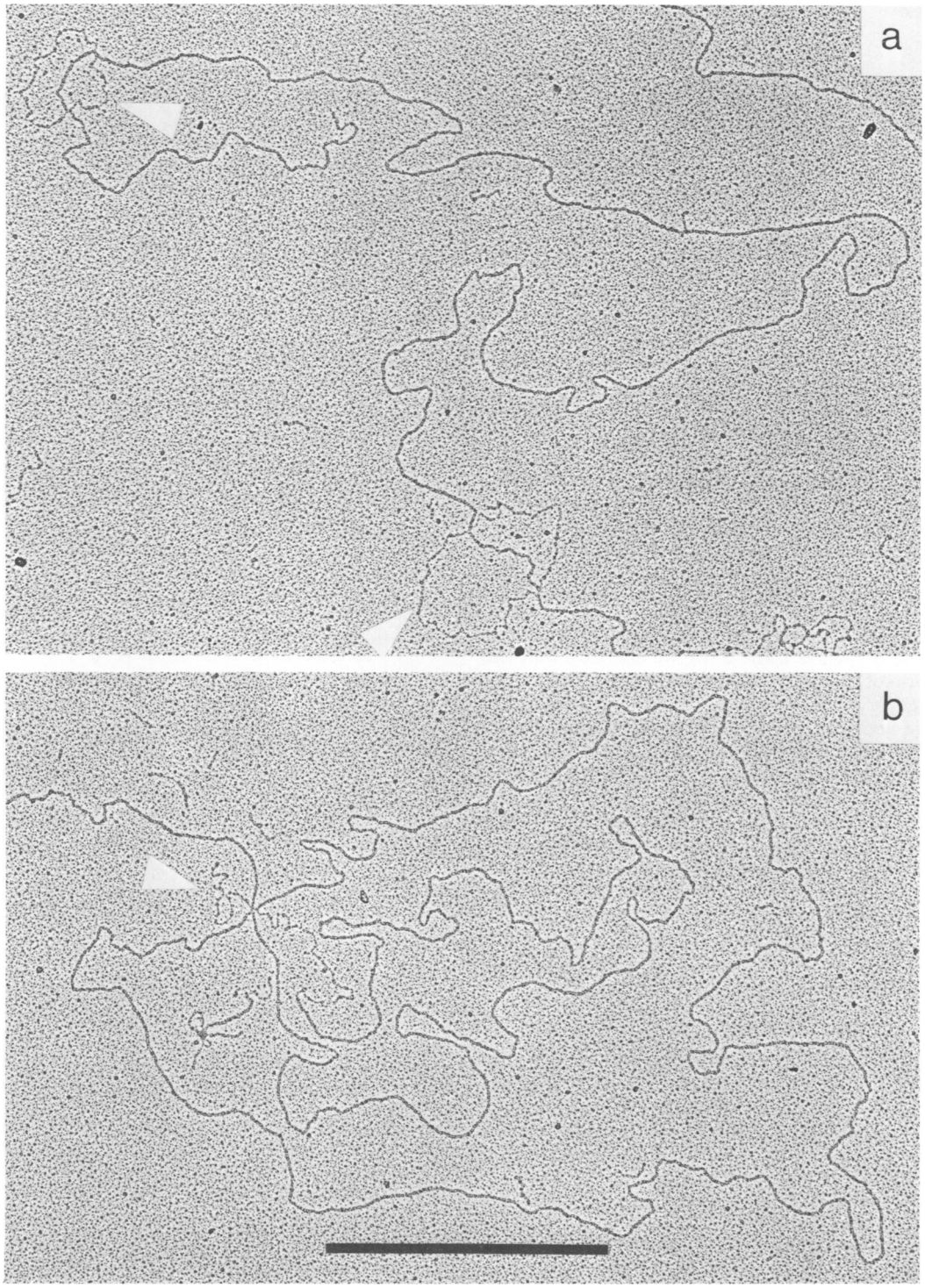

FIG. 6. *Heteroduplex formed from BF23st(4) and BF23st(9) DNAs. Nicks in DNAs extracted from BF23st(4) and BF23st(9) were ligated with T4 ligase. Ligated DNAs were mixed, denatured by formamide, allowed to renature, and prepared for electron microscopy as described in the text. Bar represents 1 μm. (a) Left end of a heteroduplex molecule showing two single-stranded deletion loops (arrows). (b) Right end of the same molecule shown in (a). Arrow indicates a single-stranded end. The central portion of the molecule which is not shown is all double-stranded.*

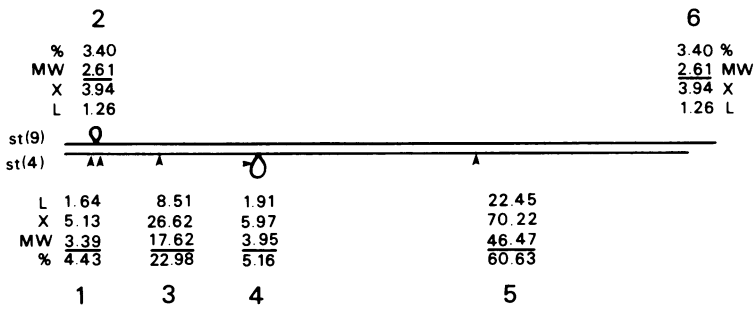

FIG. 7. *Map of heteroduplex DNA molecules such as those shown in Fig. 6. The upper line represents the intact single strand of DNA from BF23st(9). The lower line represents the ligated single strand of DNA from BF23st(4). Arrows indicate the locations of major nicks as they occur in BF23(+) (see Fig. 4). Heteroduplex regions are numbered 1 through 6; their sites are given in micrometers (L), kilobase pairs (X), molecular weight (in millions) of double-stranded DNA (MW), and percentage of total BF23(+) chromosome length (%).*

were isolated and examined by both sedimentation in sucrose density gradients and electron microscopy. Figure 8 shows the result of sedimentation in sucrose gradients. From the relationship, $\frac{D_2}{D_1} = \left(\frac{M_2}{M_1}\right)^{0.35}$, between distance sedimented (D) and molecular weight (M) for molecular species 1 and 2 (5), we estimate that the ratio of the molecular weight of FST DNA from BF23*st*(4) to that from BF23(+) is 0.66. Measurements of the contour lengths of the isolated FST DNA from BF23(+) and BF23*st*(4) by electron microscopy confirm this ratio and indicate the molecular weights of the FST DNA as 6.2 $\times$ 10^6 from BF23(+) and as 4.0 $\times$ 10^6 from BF23*st*(4) (Table 2; Fig. 9). These results are entirely compatible with a deletion in the terminal redundancies of BF23*st*(4) DNA of a size determined by heteroduplex mapping. The results also suggest a mechanism by which DNA transfer is temporarily halted after the FST DNA has been transferred (see below).

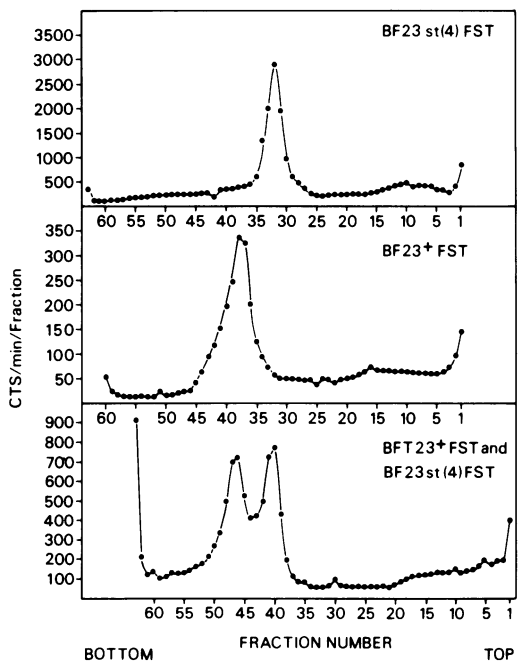

FIG. 8. *Sucrose density gradient sedimentation of FST DNA from BF23(+) and BF23st(4). FST DNAs from BF23(+) and BF23st(4) were prepared and sedimented as described in the text. Sedimentation of the mixture of the two FST DNAs, shown in the lowest profile, was for a longer period of time than either one alone. The profile is therefore shifted to the right to align the peaks.*

DISCUSSION

The results presented here demonstrate that BF23 DNA can be deleted, without affecting viability in common laboratory hosts, in a region different from that reported for viable deletion mutants of T5 (25). Viable deletion mutants of T5 have all involved the region from 0.216 to 0.324 of the fractional length from the left end of the T5 DNA molecule, and, as expected from the close relationship between BF23 and T5, we have shown here that viable deletion mutants of BF23 may also involve this same region. However, viable deletion mutants involving regions in the terminally redundant ends of BF23 DNA, which have not heretofore been reported for either BF23 or T5, are reported here. The only previous report of deletions in the terminally redundant ends of DNA from either BF23 or T5 is of a nonviable mutant of T5, in which one of the terminally redundant ends has been deleted entirely (24). Since viable deletions can occur in the redundant ends of BF23, some of the pre-

TABLE 2. *Contour lengths of FST DNA from BF23(+) and BF23st(4)*[a]

Source of DNA	Length			Fraction of BF23(+) DNA			Mol wt		
	(μm)	± SSD	± SDM	%	± SSD	± SDM	Millions	± SSD	± SDM
BF23(+)-FST	2.98	0.30	0.03	8.0	0.8	0.1	6.2	0.6	0.1
BF23*st*(4)-FST	1.94	0.19	0.02	5.2	0.5	0.1	4.0	0.4	0.1

[a] For details see footnotes to Table 1.

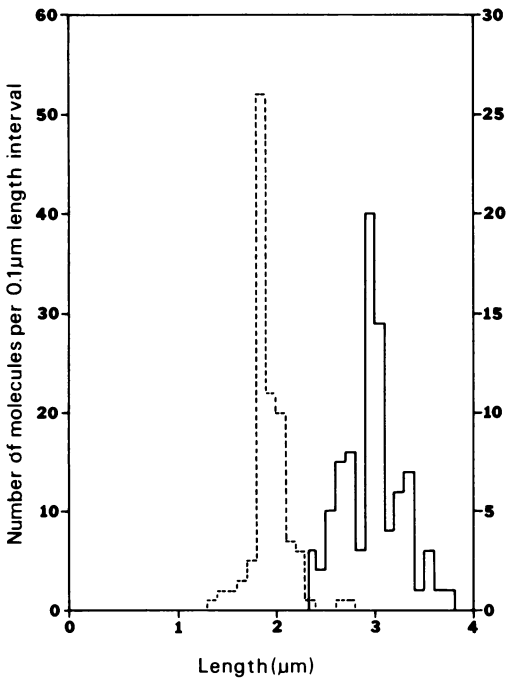

FIG. 9. *Contour lengths of FST DNA from BF23(+) and BF23st(4). FST DNAs collected from sucrose density gradients similar to those shown in Fig. 4 were prepared for electron microscopy as described in the text. Molecules measured are grouped by 0.1-μm increments. Solid line outlines the distribution of FST DNA lengths from BF23(+) . Broken line outlines the distribution of FST DNA lengths from BF23st(4).*

early proteins, which are coded by genes in the redundant ends, are dispensable, as we have reported previously (15).

An interesting question with regard to deletions from the terminally redundant ends of BF23 DNA is whether deletions from the terminally redundant ends cause the transfer of the same or different amount of DNA during the first step of DNA transfer to the host cell. The answer is that they allow transfer only of the terminally redundant DNA. This finding supports the proposal that a prime reason for the first step of DNA transfer is to inactivate certain host functions that would inactivate the large non-redundant region of BF23 DNA if DNA transfer proceeded in one step (14). In this sense the FST DNA acts as a helper phage (18). Some further support for this proposition is the finding that no cleavage sites for restriction endonucleases found in common hosts for BF23 or T5 are present in the terminally redundant ends of T5 DNA (8, 18, 27). The lack of restriction sites makes the FST DNA resistant to attack by host restriction endonucleases.

The finding that the size of the FST DNA is limited by the size of the terminal redundancy suggests to us a mechanism for this measured control of FST DNA transfer. We propose that initial transfer of DNA from phage to host stops because of a tertiary structure in the DNA at or very near the internal limit of the terminal redundancy. This tertiary structure forms as soon as the region of the DNA from which it is generated exits from the end of the phage tail attached to the host cell. The function of two pre-early proteins required for complete DNA transfer, gene product A1 and gene product A2, is to unravel this tertiary structure so that DNA transfer can proceed to completion. The possible locations in the phage DNA that generate this tertiary structure are proposed in Fig. 10. If the location is within the terminal redundancy (Fig. 10, models A and B), it must be repeated at both ends, and this requires that one redundant end cannot enter the host at all. Transfer of the

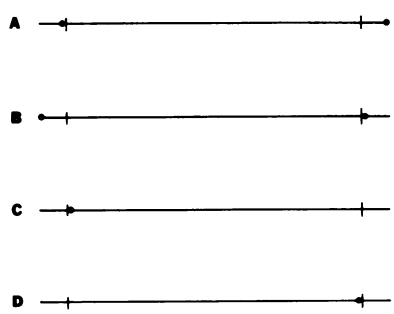

FIG. 10. *Possible locations of the structure-limiting FST. Horizontal lines represent the duplex DNA molecule of BF23. Vertical bars represent the internal limits of the terminal redundancies. Solid circles indicate possible locations of the structure that limits FST DNA.*

other redundant end would stop near the internal limit of the terminal redundancy. Such a situation would dictate that DNA transfer must proceed from one end or the other, but not randomly from either end. If the location is just outside the internal limit of the terminal redundancy and therefore in the non-redundant region (Fig. 10, models C and D), then DNA transfer must also proceed only from one end or the other. If the end distal to the stop structure were transferred first, the transfer would include the large non-redundant region of the DNA, which may then be inactivated. Furthermore, we do not find FST-DNA larger than about 6.3 Mdal (Fig. 8). Although all models predict a defined polarity of DNA transfer, they do not distinguish between right-end or left-end transfer. However, the evidence for left-end transfer is now quite convincing (22, 23) so that models A and C in Fig. 10 appear to be the most likely possibilities.

The electrophoretic patterns of single-stranded DNA fragments from denatured T5(+) and BF23(+) DNA are remarkably similar, and they emphasize once again the close relationship between these two phages. The major nicks are all in very similar if not identical locations along the DNA of both BF23 and T5. One nick in BF23, the seventh from the left end of the DNA molecule shown in Fig. 4, occurs more frequently in BF23 DNA than in T5 DNA and is at a significantly different location. However, the main difference in the pattern and frequency of nicks occurs in the terminal redundancies. In T5, minor nicks have been located by Rhoades (20) that subdivide the left and right terminal redundancies. Of the possible single-stranded fragments generated by these nicks, four are minor and a fifth is considered a major fragment that is located by hybridization at the extreme left of the terminal redundancies (6). In BF23, on the other hand, we detected four single-stranded fragments which appear with equal frequency as estimated by fluorescence with ethidium bromide. The pattern of nicks in the terminal redundancies of BF23 DNA has not been determined as it has for T5. We have proposed a pattern for them here based upon a rough analogy to the pattern of nicks in T5 terminal redundancies and upon the molecular weights of the BF23 fragments. This proposed pattern explains the data in this paper quite well, but a closer examination of the position and frequency of nicks in the terminal redundancies of BF23 DNA is needed and is currently underway in this laboratory.

ACKNOWLEDGMENTS

This work was supported by Public Health Service research grant AI 13166 from the National Institute of Allergy and Infectious Diseases and grant GM 20851 from the National Institute of General Medical Sciences and by grant BMS76-00896 from the National Science Foundation.

LITERATURE CITED

1. **Adams, M. H.** 1953. The genotypically and phenotypically heat-resistant forms in the T5 species of bacterial phage. Ann. Inst. Pasteur Paris **84**:164-174.
2. **Adams, M. H.** 1959. Bacteriophages. Interscience Publishers, Inc., New York.
3. **Adams, M. H., and K. G. Lark.** 1950. Mutation to heat resistance in coliphage T5. J. Immunol. **64**:335-347.
4. **Bujard, H.** 1969. Location of single-stranded interruptions in the DNA of bacteriophage T5+. Proc. Natl. Acad. Sci. U.S.A. **62**:1167-1174.
5. **Burgi, E., and A. D. Hershey.** 1962. Specificity and concentration limit in self-protection against mechanical breakage of DNA. J. Mol. Biol. **4**:313-315.
6. **Chen, C.** 1976. Transcription map of bacteriophage T5. Virology **74**:116-127.
7. **Davis, R. W., M. Simon, and N. Davidson.** 1971. Electron microscope heteroduplex methods for mapping regions of base sequence homology in nucleic acids. Methods Enzymol. **21**:413-428.
8. **Hamlett, N. V., B. Lange-Gufstafson, and M. Rhoades.** 1977. Physical map of the bacteriophage T5 genome based on the cleavage products of the restriction endonucleases *Sal*I, *Sma*I, *Bam*I, and *Hpa*I. J. Virol. **24**:249-260.
9. **Hayward, G. S., and M. G. Smith.** 1972. The chromosome of bacteriophage T5 I. Analysis of the single-stranded DNA fragments by agarose gel electrophoresis. J. Mol. Biol. **63**:383-395.
10. **Hertel, R., L. Marchi, and K. Muller.** 1962. Density mutants of phage T5. Virology **18**:576-581.
11. **Jacquemin-Sablon, A., and C. C. Richardson.** 1970. Analysis of the interruptions in bacteriophage T5 DNA. J. Mol. Biol. **47**:477-493.
12. **Lang, D., and M. Mitani.** 1970. Simplified quantitative electron microscopy of biopolymers. Biopolymers **9**: 373-379.
13. **Lang, D., A. R. Shaw, and D. J. McCorquodale.** 1976. Molecular weights of DNA from bacteriophages T5, T5*st*(0), BF23, and BF23*st*(4). J. Virol. **17**:296-297.
14. **McCorquodale, D. J.** 1975. The T-odd bacteriophages. Crit. Rev. Microbiol. **4**:101-159.
15. **McCorquodale, D. J., A. R. Shaw, P. K. Shaw, and G. Chinnadurai.** 1977. Pre-early polypeptides of bacteriophages T5 and BF23. J. Virol. **22**:480-488.
16. **Mizobuchi, K., and D. J. McCorquodale.** 1971. Abortive infection by bacteriophage BF23 due to the colicin Ib factor I. Genetic studies of non-restricted and amber mutants of bacteriophage BF23. Genetics **68**:323-340.
17. **Neidhardt, F. C., P. L. Bloch, and D. F. Smith.** 1974. Culture medium for enterobacteria. J. Bacteriol. **119**: 736-747.
18. **Rabussay, D., and E. P. Geiduschek.** 1977. Regulation of gene action in the development of lytic bacteriophages, p. 1-196. *In* H. Fraenkel-Conrat, and R. R. Wagner (ed.), Comprehensive virology, vol. 8. Plenum Press, New York.
19. **Rhoades, M.** 1975. Cleavage of T5 DNA by the *Escherichia coli* R_1 restriction endonuclease. Virology **64**: 170-179.
20. **Rhoades, M.** 1977. Localization of single-chain interruptions in bacteriophage T5 DNA II. Electrophoretic studies. J. Virol. **23**:737-750.
21. **Rhoades, M., and E. A. Rhoades.** 1972. Terminal repetition in the DNA of bacteriophage T5. J. Mol. Biol. **69**:187-200.
22. **Saigo, K.** 1975. Tail-DNA connection and chromosome structure in bacteriophage T5. Virology **68**:154-165.

23. **Saigo, K.** 1975. Denaturation mapping and chromosome structure in bacteriophage T5. Virology **68**:166–172.
24. **Saigo, K.** 1976. A new bacteriophage T5 particle with a DNA lacking the terminal repetition at the 'right-hand' end. J. Mol. Biol. **107**:369–378.
25. **Scheible, P. R., and M. Rhoades.** 1975. Heteroduplex mapping of heat-resistant deletion mutants of bacteriophage T5. J. Virol. **15**:1276–1280.
26. **Scheible, P. P., E. A. Rhoades, and M. Rhoades.** 1977. Localization of single-chain interruptions in bacteriophage T5 DNA I. Electron microscopic studies. J. Virol. **23**:725–736.
27. **von Gabain, A., G. S. Hayward, and H. Bujard.** 1976. Physical mapping of the *Hind* III, *Eco* RI, *Sal* and *Sma* restriction endonuclease cleavage fragments from bacteriophage T5 DNA. Mol. Gen. Genet. **143**:279–290.